Magnetic and Electrochemical Properties of Transition Metal Complexes with Multiple Metal-to-Metal Bonds. V.[1] $[Re_2(C_6H_5COO)_4]^{n+}$ with $n = 1$ and 2, and $[Re_2Cl_4\{P(C_2H_5)_3\}_4]^{n+}$ with $n = 0, 1$, and 2

F. Albert Cotton* and Erik Pedersen

Contribution from the Department of Chemistry, Texas A&M University, College Station, Texas 77843. *Received June 19, 1974*

Abstract: Rotating disk electrode polarography and cyclic voltammetry have shown that the reaction $[Re_2(C_6H_5COO)_4]^{2+} + e^- \rightleftarrows [Re_2(C_6H_5COO)_4]^+$ is quasi-reversible in dichloromethane and acetonitrile solutions at 25° with $E_{1/2} = -0.28$ and -0.26 V *vs.* sce, respectively. The reactions $[Re_2Cl_4\{P(C_2H_5)_3\}_4]^{2+} + e^- \rightleftarrows [Re_2Cl_4\{P(C_2H_5)_3\}_4]^+$ and $[Re_2Cl_4\{P(C_2H_5)_3\}_4]^+ + e^- \rightleftarrows [Re_2Cl_4\{P(C_2H_5)_3\}_4]$ are quasi-reversible in dichloromethane solutions at 25° with $E_{1/2} = 0.87$ and -0.36 V *vs.* sce, respectively. Under these conditions all the complexes have lifetimes exceeding 300 sec. The phosphine complexes constitute the first described series of multiply bonded dinuclear metal complexes, having three stable oxidation numbers. The frozen solution esr spectra at X- and Q-band frequencies of the complexes with one positive charge are interpreted in terms of one unpaired electron with hyperfine coupling to two equivalent rhenium nuclei with $I = 5/2$. The parameters obtained for $[Re_2(C_6H_5COO)_4]^+$ are: $g_\parallel = 1.713$, $g_\perp = 2.136$, $|A_\parallel| = 573 \times 10^{-4}$ cm^{-1}; and $|A_\perp| = 272 \times 10^{-4}$ cm^{-1}. The spectra of $[Re_2Cl_4\{P(C_2H_5)_3\}_4]^+$ are less informative, probably because of hyperfine splittings from the four ^{31}P. The following approximate parameters were obtained: $g_\parallel < 2$, $g_\perp \approx 2.25$, $|A_\perp^{Re}| \approx 1.6 \times 10^{-2}$ cm^{-1}, and $|A_\perp^{P}| \approx 9 \times 10^{-3}$ cm^{-1}. The other complexes give no esr signals, and they are probably diamagnetic. The g factors of dinuclear molybdenum, technetium, and rhenium complexes with the average oxidation number 2.5 and having spin-doublet ground states are qualitatively correlated with preliminary one-electron energy diagrams based on MO and scattered wave Xα calculations. The esr data tend to be in favor of the Xα calculations.

Since the discovery of the quadruple bond in $Re_2Cl_8^{2-}$ in 1964[2,3] a large number of compounds containing such a bond[3] or other multiple M-M bonds[4] has been described in the literature.[5] The structural aspect of the subject has been rather fully developed with over 30 crystallographic structure determinations, and the preparative and reaction chemistry are also extensively described. The aspects most in need of investigation have been the redox chemistry, magnetic properties of the species with unpaired electrons, and the detailed electronic structures of the compounds. At present activities in this laboratory are directed mainly along these last-mentioned three lines. Four recent publications[1,6-8] have described some of our work of this kind. In this paper we report further observations and attempt to interpret these and the earlier ones in terms of a description of the bonding.

Experimental Section

The instruments used in the investigations reported here have been described in detail in part I of this series.[1]

Thanks are due to Mr. L. Shive for the preparation of $[Re_2(C_6H_5COO)_4]Cl_2{\cdot}2CHCl_3$, according to the procedures earlier described,[9,10] and to Mr. J. R. Ebner, Purdue University, for the preparation of two of the samples of $[Re_2Cl_4\{P(C_2H_5)_3\}_4]$.[11]

Results

Electrochemistry of $[Re_2(C_6H_5COO)_4]Cl_2$. Rotating disk electrode polarograms were recorded for approximately 10^{-4} *M* solutions in 0.1 *M* tetrabutylammonium perchlorate in dichloromethane and acetonitrile solutions at 25 ± 1°. The potential ranges covered were -1.5 to 0.5 and -2 to 2 V *vs.* sce, respectively. For both solvents two-wave reduction reactions were observed. The corresponding potentials were approximately -0.3 and -1.1 V *vs.* sce. The last reduction reaction occurred over a wide potential range and had limiting currents with no simple relation either to the rate of rotation or to the limiting current of the first reduction step. For the first reduction reaction $i_L/\sqrt{\omega}$ was independent of ω, where i_L is the limiting current and ω is the cyclic frequency of rotation, for rotation rates between 1 and 50 sec^{-1} and a potential sweep rate of 5 mV sec^{-1}. Plots of E *vs.* log $(i_L - i)/i$ had slopes of 60 ± 1 mV for rotation rates below 20 sec^{-1} in acetonitrile and below 5 sec^{-1} in dichloromethane. The values of $E_{1/2}$ in the two solvents were -0.26 and -0.28 V *vs.* sce, respectively. For platinum, gold, and carbon the potentials were independent of the electrode material.

Cyclic voltammetry showed that the first-formed reduction product has a lifetime of the order of minutes. Typical voltammograms for acetonitrile solutions are shown in Figure 1. If the switching potential was between the two values of $E_{1/2}$ as in Figure 1A, then the reaction with $E_{1/2} = -0.26$ V *vs.* sce showed $i_p^a/i_p^c = 1$ for sweep rates between 2 and 200 mV sec^{-1}. The potential separation between the anodic and cathodic peaks varied with the sweep rate, ν, as expected for a quasi-reversible electron transfer,[12] giving values of $\Psi\sqrt{\nu} = 0.15 \pm 0.01$ V$^{1/2}$ sec$^{-1/2}$ independent of ν. The quantity $i_p/\sqrt{\nu}$ was independent of ν for all sweep rates. The second reduction reaction taking place at approximately -1.1 V *vs.* sce is irreversible as seen from Figure 1B. The question whether this irreversibility was caused by very slow electron transfer or by the presence of overlapping reductions leading to chemically unstable compounds remains unanswered. This second reduction peak showed no simple variation with the potential sweep rate.

Cyclic voltammetry in dichloromethane solutions gave qualitatively similar voltammograms which had $E_{1/2} = -0.28$ V *vs.* sce and $\Psi\sqrt{\nu} = 0.04$ V$^{1/2}$ sec$^{-1/2}$.

The exact composition of the rhenium complexes present in solutions of $[Re_2(C_6H_5COO)_4]Cl_2$ is uncertain. The crystal structure of the brick red chloroform adduct[13] showed that the chloride ions are coordinated at the axial positions in the rhenium dimers, but with Re-Cl bonds (2.49 Å) longer than normally observed for rhenium(III) complexes, *viz.*, 2.35 Å. We suggest that the dichloro complex is only slightly dissociated in the brick red solutions in dichloromethane but highly dissociated in the yellow-orange acetonitrile solutions. This was qualitatively supported by conductivity measurements. This may explain the small

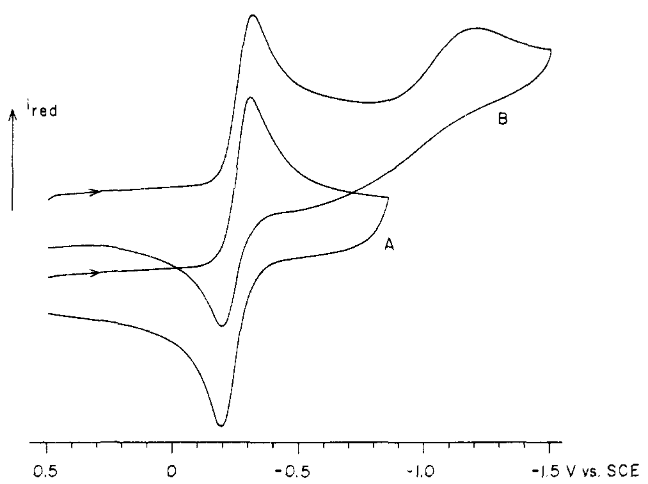

Figure 1. Cyclic voltammograms of $[\mathrm{Re_2(C_6H_5COO)_4}]^{2+}$ in acetonitrile, 0.1 *M* in tetrabutylammonium perchlorate. Potential sweep rate 100 mV $\mathrm{sec^{-1}}$. The only difference between A and B is the switching potential.

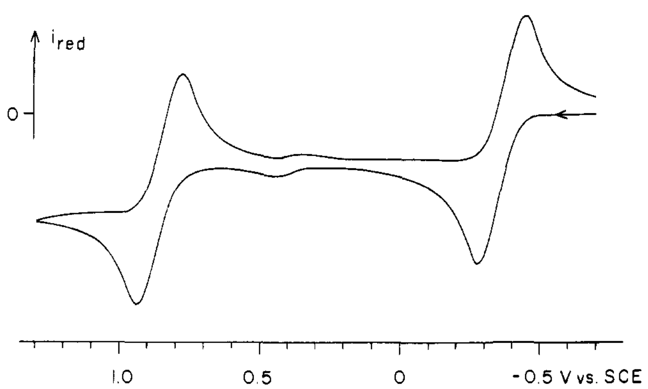

Figure 2. Cyclic voltammogram of $[\mathrm{Re_2Cl_4\{P(C_2H_5)_3\}_4}]$ in dichloromethane, 0.1 *M* in tetrabutylammonium perchlorate. Potential sweep rate 40 mV $\mathrm{sec^{-1}}$. The small wave at ~0.4 V *vs.* sce is caused by an impurity.

difference in $E_{1/2}$ values and the much lower value of $\Psi\sqrt{\nu}$ found in dichloromethane. No additional information on the kinetics of the possible dissociation reaction required prior to the electron transfer could be obtained from cyclic voltammetry. We found, however, that addition of excess chloride ions to the dichloromethane solutions (approximately 0.1 *M* in chloride) inhibits the reduction at this potential and leads to a series of irreversible reductions at more negative potentials. We interpret these results in terms of reaction scheme 1.

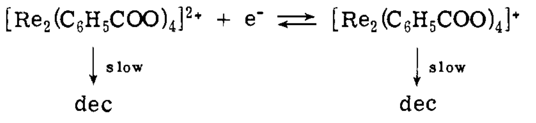

$$\begin{array}{ccc} [\mathrm{Re_2(C_6H_5COO)_4}]^{2+} + e^- & \rightleftharpoons & [\mathrm{Re_2(C_6H_5COO)_4}]^{+} \\ \downarrow \text{slow} & & \downarrow \text{slow} \\ \text{dec} & & \text{dec} \end{array} \qquad (1)$$

The novel yellow complex with an average oxidation number of 2.5 could be generated electrolytically at −0.5 V *vs.* sce in solutions. It appeared to be stable for hours since cyclic voltammograms remained unchanged with time. Such solutions were used for recording of the esr spectra.

Electrochemistry of $[\mathrm{Re_2Cl_4\{P(C_2H_5)_3\}_4}]$. Redox reactions of this complex at 25 ± 1° in dichloromethane and acetonitrile solutions containing 0.1 *M* tetrabutylammonium perchlorate were studied by application of the same techniques as discussed in the previous section. Rotating disk electrode polarograms showed the presence of two consecutive oxidation reactions having equal limiting currents (for all samples of the complex tried). The shapes of these polarograms were strongly dependent on the rate of rotation in the way expected for moderately slow electron transfer reactions. For $\nu = 10$ mV $\mathrm{sec^{-1}}$ and rotation rates below 2 $\mathrm{sec^{-1}}$ both steps gave rise to plots of E *vs.* $\log (i_{\mathrm{L}} - i)/i$ having slopes of 60 ± 1 mV as expected for transfer of one electron. The kinetics of the two steps seemed almost identical. The values of $E_{1/2}$ found were −0.36 and +0.87 V *vs.* sce in dichloromethane, and −0.35 and +0.66 V *vs.* sce in acetonitrile.

Cyclic voltammetry on dichloromethane solutions showed two oxidation reactions with equal peak currents and having $i_{\mathrm{p}}^{\mathrm{c}}/i_{\mathrm{p}}^{\mathrm{a}} = 1$ and $i_{\mathrm{p}}/\sqrt{\nu}$ independent of ν between 5 and 500 mV $\mathrm{sec^{-1}}$. It was found that $\Psi\sqrt{\nu} = 0.06 \pm 0.01$ $\mathrm{V^{1/2}\ sec^{-1/2}}$ for each step. The values of $E_{1/2}$ were in agreement with the results from rotating disk electrode experiments. A typical voltammogram is shown in Figure 2.

Cyclic voltammetry on acetonitrile solutions showed that the first oxidation reaction was quasi-reversible with $E_{1/2} = -0.35$ V *vs.* sce and $\Psi\sqrt{\nu} = 0.13$ $\mathrm{V^{1/2}\ sec^{-1/2}}$ for ν between 10 and 100 mV $\mathrm{sec^{-1}}$. The second oxidation reaction, however, was irreversible for all ν between 10 and 500 mV $\mathrm{sec^{-1}}$. The oxidation peak had the shape expected for a reversible reaction; the values of $i_{\mathrm{p}}^{\mathrm{a}}/\sqrt{\nu}$ and $E_{\mathrm{p}}^{\mathrm{a}} = 0.72$ V *vs.* sce were independent of ν. We feel that this is an indication of rapid decomposition of the oxidized product.

The results are summarized in the reaction schemes 2 and 3. In eq 2, $E_{1/2} = 0.87$ V *vs.* sce and $k \ll 3.10^{-3}$ $\mathrm{sec^{-1}}$

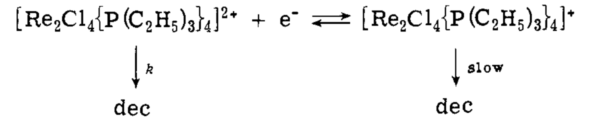

$$\begin{array}{ccc} [\mathrm{Re_2Cl_4\{P(C_2H_5)_3\}_4}]^{2+} + e^- & \rightleftharpoons & [\mathrm{Re_2Cl_4\{P(C_2H_5)_3\}_4}]^{+} \\ \downarrow k & & \downarrow \text{slow} \\ \text{dec} & & \text{dec} \end{array} \qquad (2)$$

in dichloromethane, and $E_{1/2} \approx 0.7$ V *vs.* sce and $k > 1$ $\mathrm{sec^{-1}}$ in acetonitrile. In eq 3 $E_{1/2} = -0.36$ and −0.35 V *vs.* sce in dichloromethane and acetonitrile, respectively.

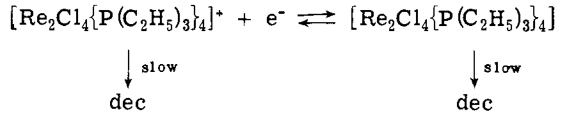

$$\begin{array}{ccc} [\mathrm{Re_2Cl_4\{P(C_2H_5)_3\}_4}]^{+} + e^- & \rightleftharpoons & [\mathrm{Re_2Cl_4\{P(C_2H_5)_3\}_4}] \\ \downarrow \text{slow} & & \downarrow \text{slow} \\ \text{dec} & & \text{dec} \end{array} \qquad (3)$$

The greenish yellow $[\mathrm{Re_2Cl_4\{P(C_2H_5)_3\}_4}]^+$ ion was generated electrolytically in dichloromethane solution at a rotating disk platinum electrode at a potential of 0.0 V *vs.* sce. These solutions, having cyclic voltammograms invariant with time, seemed stable for hours and were used for recording of the esr spectra. Similar solutions of the 2+ ion generated at 1.0 V *vs.* sce were less stable. No quantitative measurements of the lifetime were attempted.

Concluding Comments on the Redox Reactions. The potentials and lifetimes found in the present investigation together with the previously obtained information[5] on the one-electron reduction of $[\mathrm{Re_2Cl_8}]^{2-}$ tend to indicate that oxidation numbers of rhenium lower than 3 in dinuclear complexes are stabilized by chelate ligands as also found for corresponding molybdenum complexes.[1,7] The general tendency of phosphine ligands to stabilize lower oxidation numbers is also clearly demonstrated.

Esr Spectra of $[\mathrm{Re_2(C_6H_5COO)_4}]^+$. Solid salts of this complex have not been isolated, and reasonably accurate measurements of the magnetic susceptibility could therefore not be obtained. Frozen solution esr spectra of approximately 10^{-3} *M* dichloromethane solutions, 0.1 *M* in tetrabutylammonium perchlorate, at 77 K were recorded at X- and Q-band frequencies. This solvent has a strong tendency to crystallize, even when very rapidly cooled, but it was sometimes possible to obtain glasses. Interestingly, the crystallization had only a very small effect on the esr spectra.

The spectra of the glasses showed extraordinarily good resolution; typical examples are shown in Figures 3 and 4.

Computer simulation of esr spectra of axially symmetric molecules with a single unpaired electron having hyperfine coupling to two equivalent nuclei has been discussed in part I of this series.[8] The almost ideal D_{4h} symmetry of the $[Re_2(C_6H_5COO)_4Cl_2]$ complex in the crystal lattice[13] is expected to persist in $[Re_2(C_6H_5COO)_4]^+$ in solution. Naturally occurring rhenium consists of the isotopes ^{185}Re and ^{187}Re. Dinuclear complexes will thus consist of the three nuclear isomers tabulated in Table I. For an axially symmetric complex with $S = \frac{1}{2}$ and $I^{(1)} = I^{(2)} = \frac{5}{2}$ there would be expected 36 weak parallel orientation lines and 36 strong perpendicular orientation lines each split into a triplet because of the different μ values of the two rhenium isotopes. Additional intermediate orientation lines may be present.

Table I. Isotopic Isomers of Dinuclear Rhenium Complexes Based on the Naturally Occurring Isotope Ratio

Composition	% abundance	$I^{(1)}$	$I^{(2)}$	$\mu^{(1)}$	$\mu^{(2)}$
$^{185}Re-^{185}Re$	13.74	$^5/_2$	$^5/_2$	3.172	3.172
$^{185}Re-^{187}Re$	46.66	$^5/_2$	$^5/_2$	3.172	3.204
$^{187}Re-^{187}Re$	39.60	$^5/_2$	$^5/_2$	3.204	3.204

The X-band spectrum in Figure 3 partly shows such a pattern. We interpret the series of relatively intense lines in the range 1550-4175 G as perpendicular orientation lines with the outer two lines ascribed to $J = I^{(1)} + I^{(2)} = 5$. At the low-field end of this part of the spectrum the triplet splitting is clearly revealed. Parallel orientation lines are observed from 450 G and up. The lines become broader and weaker at higher fields. The triplet pattern is evident in the three low-field lines. The relative intensities of the components of each triplet, 39.6:47.5:13.6, as well as their relative positions are in excellent agreement with predictions made from Table I. Such a pattern can only be simply explained in terms of hyperfine coupling to two equivalent rhenium nuclei. We assign these sets of lines at 450, 980, and 1145 G as $H(5,-5,0)$, $H(5,-4,0)$, and $H(4,-4,0)$, respectively, in the notation $H(J,M_J,\theta)$. From this assignment the negative peak of the line $H(5,5,0)$ is expected around 7000 G. No lines could, however, be distinguished from noise above 5400 G, but the pattern revealed below this field shows that this is still in a range of close-lying components of different J values, as expected.

As a first approximation the spin Hamiltonian parameters obtained from this assignment are: $g_\parallel \approx 1.7$, $g_\perp \approx 2.2$, $|A_\parallel| \approx 700$ G, and $|A_\perp| \approx 260$ G. These values are outside the ranges where the second-order diagonalization of the spin Hamiltonian energy matrix is a sufficiently good approximation.[8]

At Q-band frequencies the second-order corrections, which also depend on J, are approximately four times smaller. The simple 11-line pattern that is expected in the high-frequency limit begins to appear in the perpendicular orientation lines, as may be seen in Figure 4. However, splittings into different J components are still observed. The second-order corrections are smaller for the parallel orientation lines, and they show no splitting into different J components. The preliminary parameters obtained from the X-band spectrum suggested the presence of two parallel orientation lines above 17,000 G in the Q-band spectrum. This is, however, beyond the limit of our spectrometer. The line at lowest magnetic field is expected around 11,000 G and can therefore not be distinguished from the more intense perpendicular orientation lines here. This leaves an ambiguity in the numbering of the parallel orientation lines and therefore in the value of $g_\parallel$. The shape of the line at 10,333 G turned out to be very sensitive to this numbering, however, as shown by computer simulation of this part of the spectrum. This line consists of contributions from $H(5,-5,\pi/2)$ and intermediate orientations where $\partial H(5,-5,\theta)/\partial H = 0$ corresponding to a minimum field. Changing the assignment $H(J,0,0)$ of the line at 14,600 G to $H(J,-1,0)$ requires the positive peak of the line at 10,333 G to be much more intense than the negative peak. The assignment $H(J,1,0)$ would require the intermediate orientation contribution to occur at 10,240 G, well separated from the perpendicular contribution. Our final assignment is shown in Figure 4, indicating the calculated positions of the I and M_J components. The corresponding spin Hamiltonian parameters are tabulated in Table II.

The line at 10,333 G and all lines above 12,000 G are nicely reproduced in computer-simulated spectra, assuming

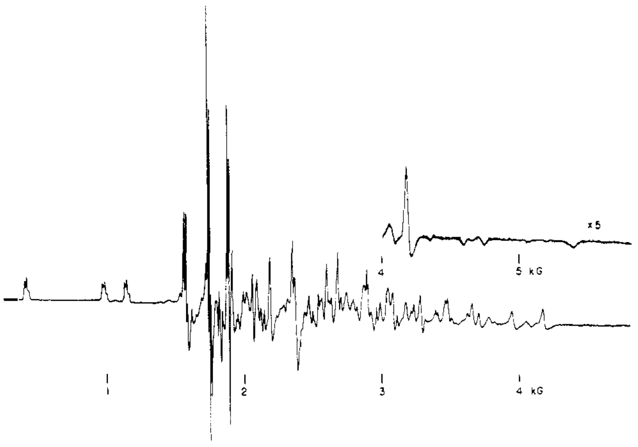

Figure 3. Frozen solution esr spectrum of $[Re_2(C_6H_5COO)_4]^+$, approximately 10^{-3} M in dichloromethane solution at 77 K. Microwave frequency 9.085 GHz.

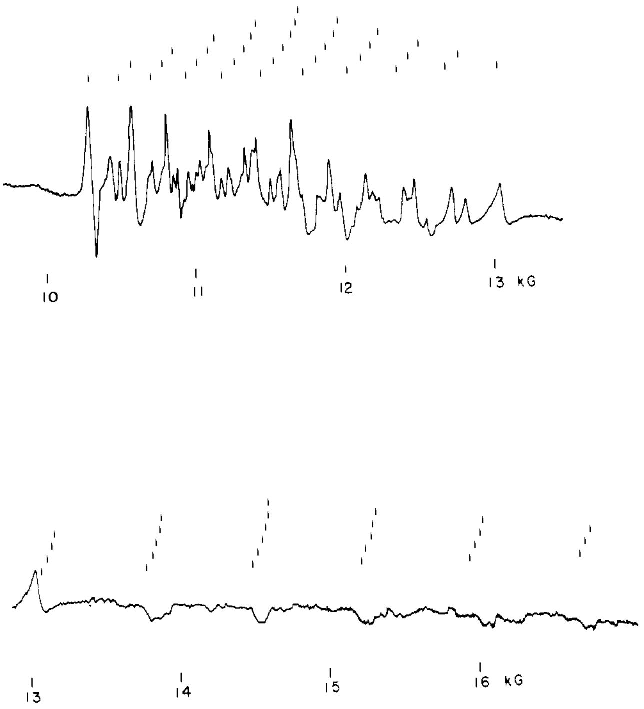

Figure 4. Esr spectrum of the same solution as in Figure 3. Microwave frequency 35.16 GHz. The lines above the upper and lower parts of the spectrum correspond to calculated line positions according to the parameters in Table II for perpendicular and parallel orientation lines, respectively. The horizontal rows of lines correspond to separate values of $J = I^{(1)} + I^{(2)}$. Only the central part of the calculated parallel orientation line pattern is shown.

Table II. Spin Hamiltonian Parameters for Dinuclear Transition Complexes with Average Oxidation Number 2.5 and $S = {}^1/_2$

Complex	$g_{\parallel}$	$g_{\perp}$	$10^4 \times |A_{\parallel}|$, cm^{-1}	$10^4 \times |A_{\perp}|$, cm^{-1}
$[Mo_2(SO_4)_4]^{3-}$ [a]	1.891	1.909	45.2	22.9
$[Mo_2(C_3H_7COO)_4]^{+}$ [b]	1.941	1.941	35.6	17.8
$[Tc_2Cl_8]^{3-}$ [c]	1.912	2.096	166	67.2
$[Re_2(C_6H_5COO)_4]^{+}$	1.71(3)	2.13(6)	573	272
$[Re_2Cl_4\{P(C_2H_5)_3\}_4$	<2	≈ 2.2	?	≈ 160

[a] Reference 7. [b] Reference 1. [c] Reference 8.

first derivative Lorentzian lines having widths of 25 G. With such widths the triplet pattern of each line is not revealed, and only one nuclear species was therefore included in the simulations. In the range 10,333–12,000 G there are so many overlapping lines that the spectrum is very dependent on even very small variations of the parameters, and no attempts were made to improve the accuracy of the parameters by fitting computer simulations to this part of the spectrum.

Esr Spectra of $[Re_2Cl_4\{P(C_2H_5)_3\}_4]^+$. A preliminary report[11] on the crystal structure of $[Re_2Cl_4\{P(C_2H_5)_3\}_4]$ has shown that the $Re_2Cl_4P_4$ skeleton has an eclipsed conformation with the point symmetry D_{2d}. The 1+ ion is likely to have the same conformation although a rapid rearrangement accompanying the electron transfer cannot be ruled out from the electrochemical data. The esr spectrum of a complex with D_{2d} symmetry is expected to show axial magnetic symmetry.

The X- and Q-band esr spectra of approximately 10^{-3} *M* frozen solutions of $[Re_2Cl_4\{P(C_2H_5)_3\}_4]^+$ in dichloromethane shown in Figures 5 and 6 have no simple patterns as observed in the spectra of the benzoate complex. The most likely reason for this is the presence of large ^{31}P hyperfine coupling, splitting each of the 216 lines expected for a rhenium dimer into quintets. Figures 5 and 6 may well be 1080-line spectra with insufficient resolution. The only information obtained from the X-band spectrum is: $g_{\parallel} < 2$, $g_{\perp} \approx 2.25$, and $|A_{\perp}^{\mathrm{Re}}| \approx 2 \times 10^{-2}\ \mathrm{cm}^{-1}$.

The Q-band spectrum shows intense lines around a field corresponding to $g_{\perp} \approx 2.23$. The four low-field lines have splittings of approximately 85 G in contrast to the 155 G found for the three following lines and for lines at higher fields. We suggest the following explanation: $|A_{\perp}^{\mathrm{P}}| \approx 85$ and $|A_{\perp}^{\mathrm{Re}}| \approx 155$ G where the axis of reference is the Re-Re axis in both cases. Since we were unable to detect any parallel orientation lines with certainty in the Q-band spectrum, we did not consider it worthwhile to attempt the refinement of these parameters *via* lengthy computer simulations based on such sparse data. The apparent low signal-to-noise ratio for our Q-band spectrometer is an artifact caused by the extreme widths of the spectra of a single electron. Sensitivity measurements with various simple compounds in frozen solutions having approximately the same dielectric properties as the solutions described above showed that the sensitivity was close to the expected value of 10^{11} spins/G.

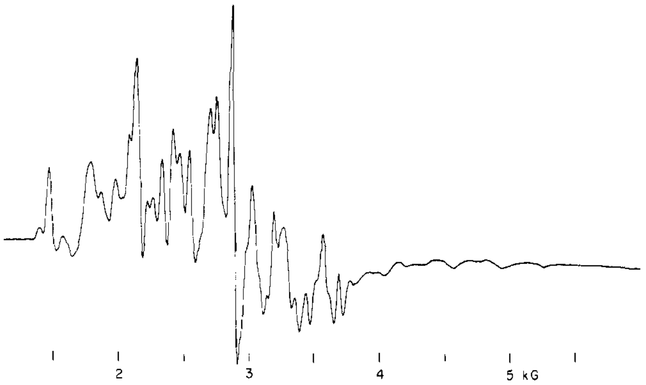

Figure 5. Frozen solution esr spectrum of $[Re_2Cl_4\{P(C_2H_5)_3\}_4]^+$, approximately 10^{-3} *M* solution in dichloromethane at 77 K. Microwave frequency 9.08 GHz.

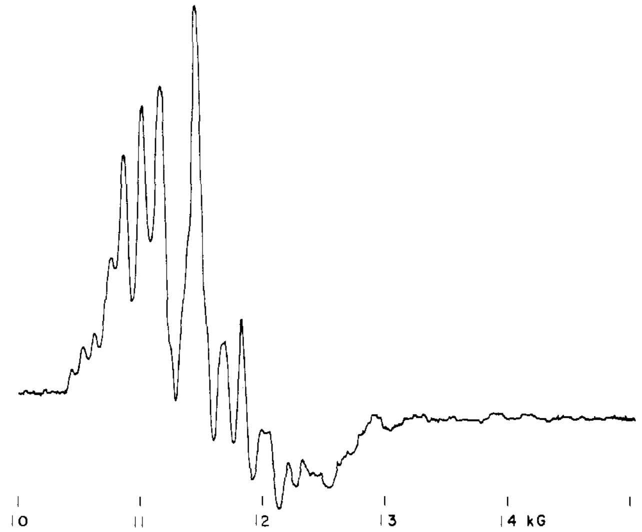

Figure 6. Esr spectrum of the same solution as in Figure 5. Microwave frequency 35.63 GHz.

Another interpretation of the esr spectra is possible but not likely to be chemically reasonable. The X-ray structure of $[Re_2Cl_4\{P(C_2H_5)_3\}_4]$ showed a highly disordered arrangement in a cubic unit cell. The assumption of molecular D_{2d} symmetry of the $Re_2Cl_4P_4$ skeleton was not based on the diffraction data but on estimates of steric hindrance. The point symmetry D_{2h} fits the diffraction data equally well. Such a molecular symmetry would give rise to rhombic magnetic symmetry. Under such an assumption the first four lines in the Q-band spectrum could show splittings different from the following lines because of a difference between $|A_x|$ and $|A_y|$. Future computer simulations may provide sufficient information to settle the questions of molecular symmetry of the 1+ ion, magnetic equivalence of the two rhenium nuclei, and the values of the ^{31}P hyperfine coupling constants.

Discussion

A sufficient body of esr results (see Table II) has now accumulated to warrant an attempt at devising a consistent interpretation in terms of possible electronic configurations for species with one unpaired eletron. According to the original qualitative description of a quadruple bond,[2b] the species we have examined should either have one vacancy in the δ bonding orbital ($Mo_2(SO_4)_4{}^{3-}$, $Mo_2(O_2CR)_4{}^+$) or have one electron in excess of the four pairs necessary to form the quadruple bond ($Tc_2Cl_8{}^{3-}$, $Re_2(O_2CR)_4{}^+$, $Re_2Cl_4(PR_3)_4{}^+$).

The theory of *g* factors at the level of second-order perturbation theory,[14] which is assumed to provide sufficient accuracy for qualitative arguments, leads to expressions 4 and 5.

$$g_{\parallel} = 2.0023 - 4\sum_n \frac{\langle\Psi_n|\mathcal{H}_{1s}|\Psi_0\rangle\langle\Psi_0|L_z|\Psi_n\rangle}{E_n - E_0} \tag{4}$$

$$g_{\perp} = 2.0023 - 4\sum_n \frac{\langle\Psi_n|\mathcal{H}_{1s}|\Psi_0\rangle\langle\Psi_0|L_y|\Psi_n\rangle}{E_n - E_0} \tag{5}$$

Ψ_0 and Ψ_n refer to the ground state and the excited states, respectively, having energies E_0 and E_n. The spin-orbit coupling operator $\mathcal{H}_{ls}$ is assumed to be of the form

$$\mathcal{H}_{1s} = \sum_k \{\sum_i \xi_i r_{ik} l_{ik}\} s_k \tag{6}$$

where the subindices refer to electron k centered at nucleus i.

In the following we shall make the most primitive correlations possible between the g factors in Table II and one-electron energy diagrams presently available. No energy calculations have been performed on systems with one unpaired electron, but crudely estimated excited state energies may be obtained from MO calculations on $[Re_2Cl_8]^{2-}$ according to Cotton and Harris[15] and from scattered wave Xα calculations on $[Mo_2Cl_8]^{4-}$ according to Norman and Kolari.[16]

According to both types of calculations the ground state of dinuclear molybdenum complexes with the average oxidation number 2.5 is $^2B_{2g}$, with the odd electron occupying an almost pure metal-metal δ-bonding orbital. For the corresponding technetium and rhenium complexes the two calculations disagree about the nature of the ground state. MO calculations suggest $^2A_{2u}$, an essentially metal centered nonbonding orbital. Xα calculations suggest $^2B_{1u}$, the metal-metal δ*-antibonding orbital.

The angular momentum operator L transforms in D_{4h} as $E_g + A_{2g}$. Contributions to the summations in eq 4 and 5 will thus depend on $\langle\Gamma_0|A_{2g}|\Gamma_n\rangle$ and $\langle\Gamma_0|E_g|\Gamma_n\rangle$ being nonzero for $g_\parallel$ and $g_\perp$, respectively.

For the molybdenum complexes with $\Gamma_0 = B_{2g}$ only excited states which transform as B_{1g} and E_g will influence $g_\parallel$ and $g_\perp$, respectively. Such excited states, mainly metal centered, are available in both energy calculations with approximately the same energy (~11 kK according to Xα calculations). It is therefore expected that $g_\parallel \approx g_\perp < 2$ as also found experimentally. If future attempts to prepare similar tungsten complexes should be successful, these are thus expected to show reduced g factors for the same reasons.

For technetium and rhenium complexes, assuming the ground state to be A_{2u} according to the MO calculations, excited states with the symmetries A_{1u} and E_u will be of importance for $g_\parallel$ and $g_\perp$, respectively. No close-lying A_{1u} states are available, and $g_\parallel = 2$ is expected. Exciting a lower lying π-bonding electron to the half-fitted A_{2u} level gives an essentially metal-centered excited state with symmetry E_u and having the approximate energy 4 eV, neglecting interelectronic repulsion effects. This gives $g_\perp > 2$. The contribution to $g_\perp$ is now positive because the interaction involves a filled excited orbital. The first of these predictions is contrary to the experimental results.

According to the Xα calculations[16] the ground state in the technetium and rhenium complexes is B_{1u}, and contributions to $g_\parallel$ and $g_\perp$ are thus expected from excited states which transform as B_{2u} and E_u, respectively. The same E_u orbital (now with energy ~11 kK, disregarding interelectronic repulsion effects) that was of importance for $g_\perp$ in the MO calculations will lead to $g_\perp > 2$. An empty B_{2u} orbital (mainly metal-centered and having the approximate energy 7 kK) will lead to $g_\parallel < 2$. These two predictions are in agreement with the experimental values. $\Delta g_\parallel$ and $\Delta g_\perp$ are larger for rhenium than for the technetium complexes in accordance with their relative spin-orbit coupling constants.

These qualitative arguments thus tend to support the results of the Xα calculations. A similar evidence is obtained from the ^{31}P hyperfine coupling constant in $[Re_2Cl_4\{P(C_2H_5)_3\}_4]^+$ ($|A_\perp^P|$ estimated to be 85 G. Such a high value is unexpected if the ground state, as found in the MO calculations, were an A_{2u} orbital having almost no electron density in the vicinity of the ^{31}P atoms. The ground state B_{1u}, according to the Xα calculations, has its maximum electron densities pointing directly toward the ligands and may for this reason explain the large ligand hyperfine coupling constant. A more detailed discussion of this, *viz.*, isotropic and anisotropic hyperfine coupling contributions, must, however, await a detailed interpretation of esr spectra of oriented molecules.

One of the chief results of the esr studies is thus to cast great doubt upon the earlier proposal[15] that in the $[Re_2Cl_8]^{2-}$ ion there is a σ-nonbonding orbital lying at the same approximate level as or below the level of the δ* orbital. Such a σ(n) orbital would have to arise from metal p_z or s orbitals, and evidently these are too high in energy to give rise to an MO at so low an energy. This is implicit in the results of Norman and Kolari.[16] There have, in fact, been earlier reasons for believing that the previous MO calculation[15] yielded incorrect results. A number of years ago an MCD study of the spectrum of the $[Re_2Cl_8]^{2-}$ ion[17] showed that the strong band at about 33 kK, previously proposed as the $\delta \rightarrow \delta^*$ transition, could not be so assigned since it exhibited an A term, indicative of a degenerate excited state. Since 33 kK was already a rather large energy for a $\delta \rightarrow \delta^*$ bond, the only alternative assignment, among the reported bands, would be to the rather weak one at 14.5 kK. This assignment had previously been eschewed mainly because such a weak band (oscillator strength of only *ca.* 10^{-2}) was considered unlikely to be due to an electronically allowed transition. Quite recently, several pieces of experimental data also suggesting this assignment have been reported, and so interpreted, by Cowman and Gray.[18] It thus appears that a bonding scheme approximating that obtained in the scattered wave Xα calculation for $[Mo_2Cl_8]^{4-}$ by Norman and Kolari[16] is the best guide now available to the electronic structures of species with quadruple bonds. Apropo, a very similar result was obtained in a more conventional MO calculation performed at the University of Wisconsin.[19]

Acknowledgments. As before, we are indebted to Professor J. H. Lunsford (TAMU) for esr facilities, the Robert A. Welch Foundation for funds to purchase the Beckman Electroscan 30, and the University of Copenhagen, Chemical Laboratory I, H. C. Ørsted Institute, Denmark, for a Leave of Absence to E.P. Finally, the generous support of the National Science Foundation under Grant No. 33142X is gratefully acknowledged.

References and Notes

(1) For Part IV, see F. A. Cotton and E. Pedersen, *Inorg. Chem.*, in press.
(2) (a) F. A. Cotton, *et al.*, *Science*, **145**, 1305 (1964); (b) F. A. Cotton, *Inorg. Chem.*, **4**, 334 (1965).
(3) (a) F. A. Cotton, *Rev. Pure Appl. Chem.*, 17, 25 (1967); (b) F. A. Cotton, *Accounts Chem. Res.*, **2**, 240 (1969); (c) P. A. Koz'min, *Dokl. Akad. Nauk SSSR*, **206**, 1384 (1972).
(4) (a) F. Huq, W. Mowat, A. Shortland, A. C. Skapski, and G. Wilkinson, *Chem. Commun.*, 1079 (1971); (b) M. H. Chisholm, F. A. Cotton, B. A. Frenz, and L. Shive, *J. Chem. Soc., Chem. Commun.*, 480 (1974); (c) M. J. Bennett, K. G. Caulton, and F. A. Cotton, *Inorg. Chem.*, **8**, 1 (1969); (d) F. A. Cotton, B. G. DeBoer, M. D. LaPrade, J. R. Pipal, and D. A. Ucko, *Acta Crystallogr., Sect. B*, **27**, 1664 (1971).
(5) An overview of the field, with extensive documentation, based upon a Centenary Lecture sponsored by the Chemical Society (London), given at British universities in Feb. 1974, by F.A.C. is in course of publication in *Chem. Soc. Rev.*
(6) F. A. Cotton and E. Pedersen, *Inorg. Chem.*, in press.
(7) F. A. Cotton, B. A. Frenz, E. Pedersen, and T. R. Webb, *Inorg. Chem.*, in press.
(8) F. A. Cotton and E. Pedersen, *Inorg. Chem.*, in press.
(9) F. A. Cotton, N. F. Curtis, B. F. G. Johnson, and R. W. Robinson, *Inorg. Chem.*, **4**, 326 (1965).
(10) F. A. Cotton, C. Oldham, and R. A. Walton, *Inorg. Chem.*, **5**, 1798 (1966).

(11) F. A. Cotton, B. A. Frenz, J. R. Ebner, and R. A. Walton, *J.C.S. Chem. Commun.*, 4 (1974).
(12) R. S. Nicholson, *Anal. Chem.*, **37**, 1351 (1965).
(13) M. J. Bennett, W. K. Bratton, F. A. Cotton, and W. R. Robinson, *Inorg. Chem.*, **7**, 1570 (1968).
(14) B. R. McGarvey, *Transition Metal Chem.*, **3**, 89 (1966).
(15) F. A. Cotton and C. B. Harris, *Inorg. Chem.*, **6**, 924 (1967).
(16) J. G. Norman and H. J. Kolari, *J. Chem. Soc., Chem. Commun.*, 303 (1974).
(17) P. N. Schatz, University of Virginia, private communication.
(18) C. D. Cowman and H. B. Gray, *J. Amer. Chem. Soc.*, **95**, 8177 (1973).
(19) R. F. Fenske, T. Block, and D. Lichtenberger, unpublished results.

Reactions of Monatomic and Diatomic Manganese with Carbon Monoxide. Matrix Infrared Spectroscopic Evidence for Pentacarbonylmanganese $Mn(CO)_5$ and the Binuclear Carbonyls $Mn_2(CO)_n$ (where $n = 1$ or 2)

H. Huber, E. P. Kündig, G. A. Ozin,* and A. J. Poë

Contributions from the Lash Miller Chemistry Laboratory and Erindale College, University of Toronto, Toronto, Ontario, Canada.

Received June 14, 1974

Abstract: The reactions of Mn atoms with $^{12}C^{16}O$ and $^{12}C^{16}O$-Ar mixtures at 10–15°K are investigated by matrix isolation infrared spectroscopy and establish the existence of pentacarbonylmanganese, $Mn(CO)_5$, having a C_{4v} square pyramidal stereochemistry. Cotton–Kraihanzel force constants are calculated for $Mn(CO)_5$ and the absorption intensities of the CO stretching modes are used to evaluate the C_{apical}–Mn–C_{eq} angle and the ratio of the axial to equatorial transition dipole moments. The spectral and bonding properties of 15-, 16-, 17-, and 18-electron valence shell pentacarbonyls are reappraised, the $Cr(CO)_5$ problem is clarified, and a simple theory is presented which rationalizes the observed stereochemical changes. Besides its reactions in the monatomic form, manganese is also shown to react as Mn_2 dimers, formed as a result of a surface diffusion effect occurring in the quasi-liquid phase during matrix deposition. The relative concentrations of mononuclear and binuclear species depend on the concentration of metal in the matrix and on the CO:Ar ratios. Using low $^{12}C^{16}O$-Ar ratios which favor Mn_2 formation, the binuclear bridged carbonyl species $Mn_2(CO)_n$ have been synthesised. Mixed $^{12}C^{16}O$-$^{12}C^{18}O$-Ar isotope experiments establish the binuclear complexes to be bridge bonded $Mn_2(CO_b)$ and $Mn_2(CO_b)_2$ and terminally bonded $Mn_2(CO_t)$ and Cotton–Kraihanzel force constants are calculated for all species. The structure and bonding of the binuclear species and their relevance to the chemisorption of CO on manganese metal films are briefly discussed.

Cocondensation reactions of transition metal atoms with small gaseous molecules at low temperatures have recently been shown to provide synthetic routes to a number of chemically interesting species which would have previously been regarded as inaccessible through conventional forms of chemical synthesis. Using these methods, species such as $Ni(N_2)_4$,[1] $Co(CO)_4$,[2] $Ni(CS)_4$,[3] $Ni(CO)_2(N_2)_2$,[4] $Pt(O_2)_2$,[5] $Pt(N_2)_3$,[6] and $Pd(N_2)_2(O_2)$[7] have been synthesised and characterized using matrix infrared and Raman methods of analysis. In most of the cocondensation reactions so far studied, the metals Ni, Pd, and Pt have received greatest attention. These are metals whose ground state atoms have no obvious tendency toward dimerization, as shown by mass spectrometric evidence[8] which establishes at least 99% monatomic metal species in the vapor above the liquid metals, and the formation of mainly *mononuclear* complexes in their matrix reactions.[9]

Recent experiments, however, with V, Cr, Mn, Co, and Cu vapors have led us to believe that under matrix cocondensation conditions, these metals can be induced to form binuclear species. In this paper we report data for the reactions of manganese vapor with carbon monoxide.

Pentacarbonylmanganese, $Mn(CO)_5$. In 1966, Bidinosti and McIntyre discovered that the pyrolysis of $Mn_2(CO)_{10}$ vapor produced appreciable concentrations of the radical $Mn(CO)_5$, detected by its mass spectrum.[10] $Mn(CO)_5^+$ was detected both from low temperature and from high temperature $Mn_2(CO)_{10}$ vaporization. The appearance potential was lower from the high temperature vapor and it was inferred that it was being produced from $Mn(CO)_5$ radicals. It could, in principle, have been formed from any excited form of $Mn_2(CO)_{10}$. A number of studies since then have proposed that it exists as an intermediate in a number of chemical reactions of $Mn_2(CO)_{10}$. Poë, *et al.*,[11] have recently suggested that the kinetics of the thermal decomposition and the reaction of oxygen with $Mn_2(CO)_{10}$ in inert solvents imply that the rate-determining step is homolytic fission of the Mn–Mn bond. Furthermore, Haines and Poë[12] have analyzed kinetic data of Bamford, *et al.*,[13] for vinyl polymerization by mixtures of $Mn_2(CO)_{10}$ and CCl_4, in terms of initiation by CCl_3 radicals produced by the reaction of $Mn(CO)_5$ radicals with CCl_4. The reaction of Br_2 with $Mn_2(CO)_{10}$ in $CHCl_3$ or cyclohexane[14] appears to proceed by a long chain reaction that is believed to involve the propagating reaction

$$Br + Mn_2(CO)_{10} \longrightarrow BrMn(CO)_5 + Mn(CO)_5$$

$$Br_2 + Mn(CO)_5 \longrightarrow Br + BrMn(CO)_5$$

At about the same time, Wiles, *et al.*,[15] produced evidence for the existence of $Mn(CO)_5$ formed in nuclear recoil reactions of ^{56}Mn with solid $Mn_2(CO)_{10}$. The recoiling ^{56}Mn atom was stabilized in the $Mn_2(CO)_{10}$ matrix as $^{56}Mn(CO)_5$ which was subsequently detected radiochemically as $I^{56}Mn(CO)_5$.

More recently still, Wojcicki and Hallock[16] have shown that the 350-nm photolysis of $Mn_2(CO)_{10}$ in THF (corresponding to the σ–σ^* transition of the Mn–Mn bond[17]) produces an orange, paramagnetic complex which on standing at ambient temperatures slowly reverts to $Mn_2(CO)_{10}$. Addition of the orange solution to I_2 in THF under nitrogen gave 30–35% $Mn(CO)_5I$[16] whereas a solution of $Mn_2(CO)_{10}$ in THF does not react with I_2 under ambient